

# Rubberized Cord Thickness Measurement Based on Laser Triangulation – Part I: Technology

**Petar B. Petrović**

Associate Professor

Faculty of Mechanical Engineering  
University of Belgrade

*Steel and textile cord coating is one of the key rubber processing technologies in tiremaking industry. Specifications are very demanding. In particular, thickness variation across the sheet profile and downstream is very difficult to fulfill. For in-process thickness measurement the most common are systems based on non-contact beta or gamma radiation sensors. Regardless of their wide use, non-contact radiation sensors possess serious drawbacks: they are measuring thickness in indirect way only, they are highly sensitive to variations of material properties, and probably the most critical one, they are potentially dangerous for both personnel and environment. Recent advances in optoelectronics have founded new alternative method for non-contact thickness measurement based on laser triangulation. Extremely delicate optical properties of fresh calendered rubber and severe environmental conditions create serious problems in implementation of this technology. This two-part paper presents a general conceptual framework for in-process laser-based thickness measurement, and proposes a new method for processing acquired sensory data based on statistical surface characterization. Proposed method is experimentally verified, and based on these results the new measuring systems are developed and implemented in industry.*

**Keywords:** *Tire manufacturing, Laser triangulation, Thickness measurement.*

## 1. INTRODUCTION

Steel and textile cord coating, i.e., cord rubberizing, is one of the key rubber processing technologies in tiremaking industry. Specifications and tolerances of rubberized cord sheets (RCS) are very demanding. In particular, thickness variation in lateral direction (across the sheet profile) and downstream, or machine direction, as well as the cord density are very difficult to fulfill.

For in-process thickness measurement the most common are systems based on non-contact beta or gamma radiation sensors. Regardless of their wide use, non-contact radioactive sensors possess serious drawbacks: they measure thickness on indirect way only, they are highly sensitive to variations of material properties, and they are potentially dangerous.

Probably, the most serious problem with radiation sensors is their inherent risk for both, personnel and environment, which consequently requires costly maintenance and produces other implications. Environmental and, more generally, societal risk that the use of radiation sensors brings to, becomes higher and higher as related regulative (concerning health, safety and working conditions) cut down permissible levels of radiation. Extensive measures carried out by companies to comply these regulatives seriously rise up

the costs, which stresses the needs for developing alternative technology - more environment and human friendly, but also, having improved measuring properties, such as better accuracy, robustness and even surface texture scanning capabilities (high space resolution), which becomes necessary in order to enhance quality of the calendering process as well as the entire quality of products having as ingredient the rubberized cord.

Optoelectronics and optical sensors that are dedicated for in-process dimensional metrology had rapid growth in past decade [1]. They were quickly introduced in industry with success. Since they offer a challenging alternative to non-contact radiation sensors, recently there were attempts of their introduction in tiremaking industry too. Unfortunately, application of optical sensors in rubber measurement is generally not so straightforward.

Laser triangulation sensors measure thickness directly and they collect data at much higher rates than radiation sensors can, with no needs for extensive and frequent recalibration. They have no inherent risk for personnel or environment too. However, specific geometrical and optical properties of rubberized cord surface generate extremely unfavorable measuring conditions (fresh calendered rubber has a highly texturized surface, composed of interlaced black and shiny areas, and usually evaporates smoke or fumes). As a result, measured data dropout and uncertainty can become unacceptably high. Therefore, standard optical sensors cannot be applied effectively using simple analogy with in-process thickness measurements carried out in other industry segments (metalworking, pulp and

---

Received: June 2007, Accepted: September 2007.

Correspondence to: Dr Petrović B. Petar, Associate Professor  
Faculty of Mechanical Engineering,  
Kraljice Marije 16, 11120 Belgrade 35, Serbia  
E-mail: pbpetrovic@mas.bg.ac.yu

paper, plastic processing, etc). To overcome this problem it is necessary to use more enhanced optical sensing systems and extensive processing of measured data.

This paper presents a general conceptual framework for in-process thickness measurement of the rubberized cord using laser triangulation sensors, and proposes a new method for processing acquired sensory data based on statistical surface characterization. This paper also presents two examples of successful application of developed technology for in-process thickness measurement and texture profile scanning for both rubberized steel and textile cord. These measuring systems are implemented in industrial environment within the more general projects of modernization of calendering lines.

## 2. TECHNOLOGY

Laser proximity sensor for thickness measurement applications is based on optical triangulation that serves as a basic concept for displacement measurement of diffuse target surface. Basic definitions are given in standard DIN 32877, 1999 - Optoelectronic Measurement of Distance, Profile and Form.

### 2.1 Optical triangulation

The optical triangulation system consists of a light source (usually visible low power semiconductor laser), condensing lens, converging imaging lens/objective and position sensitive photo detector (shown in Fig.1). A light source projects through condensing lens a spot of light on RCS surface. Since the surface of RCS is not a perfect mirror, the light will be subjected to diffusion by reflection, and thus, the light will be scattered in all directions in a hemisphere around the point D. A portion of reflected light, passing through imaging lens E, will be more or less well focused at point F. If the RCS surface in motion has a component of displacement collinear to the incident light beam, the displaced light spot D' will have displacement components in both parallel and perpendicular direction in respect to the axis of the imaging lens E. Since the imaging lens remains stationary, the component of displacement perpendicular to the imaging lens axis causes a corresponding displacement of the image F'. In the same way, another image F'' that corresponds to the new spot location D'' may be created. The displacement of the image point F is proportional to the displacement of the diffusive RCS surface, collinear to the incident light beam. In order to measure the image displacement, a position sensing photo detector must be placed along the line F'F''.

Many triangulation systems are designed with the detector perpendicular to the main axis of the imaging lens [2]. In order to keep the image in focus, the detector must be inclined at an angle  $\gamma$  as it is governed by the F'F'' line. Applying lens formula, the image distance  $b$  may be defined as:

$$b = \frac{a f_E}{a - f_E}, \quad (1)$$

where  $a$  is the object distance and  $f_E$  is the focal length of the lens. When the RCS surface is displaced to a distance  $z$  in the direction collinear with incident laser beam, the corresponding object distance  $a'$  is then:

$$a' = \sqrt{a^2 + 2az \cos \alpha + z^2}, \quad (2)$$

where  $\alpha$  denotes the angle between incident laser beam and imaging lens axis (viewing angle). The new image distance  $b'$  is defined by substituting (2) in (1). Image displacement angle  $\beta$  can be defined using equation (2):

$$\cos \beta = \frac{a^2 + a'^2 - z^2}{2aa'}, \quad (3)$$

or equivalently, concerning image displacement  $w$ :

$$\cos \beta = \frac{b^2 + b'^2 - w^2}{2bb'}. \quad (4)$$

Unknown relation between surface displacement  $z$  and image displacement  $w$  along the F'F'' line, may be derived by superimposing equations (3) and (4):

$$w = \sqrt{\frac{(a^2 + a'^2 - z^2)bb'}{aa'} - b^2 + b'^2}. \quad (5)$$

The detector inclination angle is defined by differentiating image distance vector  $b'$  for arbitrary displacement  $z$  of RCS diffusive surface. From equation (1) follows:

$$\tan \gamma = \frac{db'}{dz} = \frac{d}{dz} \left( \frac{a' f_E}{a' - f_E} \right). \quad (6)$$

It is clear from (6) and (2) that detector inclination angle is nonlinear function of RCS surface displacement.

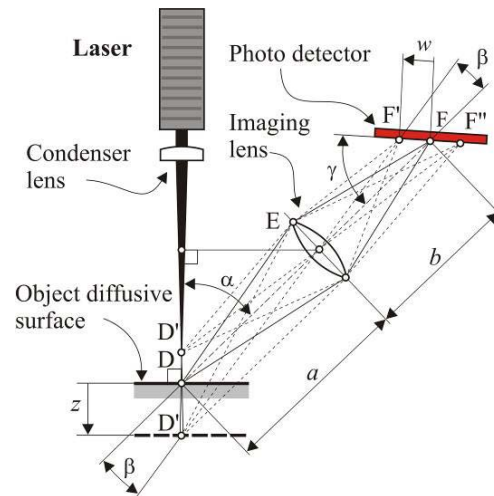


Figure 1. General outline of optical triangulation concept.

### 2.2 Photo detector

The triangulation sensors use one of two types of photo detectors to locate the center of the imaged spot: position-sensing detector (PSD) which is essentially analogue device, and one-dimensional photodiode array which is true digital device (one-dimensional CCD or CMOS imagers).

The PSD, also known as a lateral effect photodiode, is a single-element analog detector that converts incident light into continuous position data. It has three terminals, one on the back surface and two on the active front surface (shown in Fig. 2a). The active surface behaves as a very homogenous resistance, so that the current in each contact depends linearly on the light spot position, or more precisely, on the position of the light spot center of gravity. The relationship between these two output currents gives immediately the light spot position through the relation:

$$x = \frac{L}{2} \left( \frac{y_1 - y_2}{y_1 + y_2} \right), \quad (7)$$

where  $L$  is the length of the PSD active surface. It is important that the intensity of the incident light spot does not affect the calculation of the light spot position. However, relation (7) also shows that information of the light spot intensity profile is completely lost. The lost information content makes PSD sensitive to errors generated by distortion of Gaussian profile of the imaged light spot (Fig. 2b).

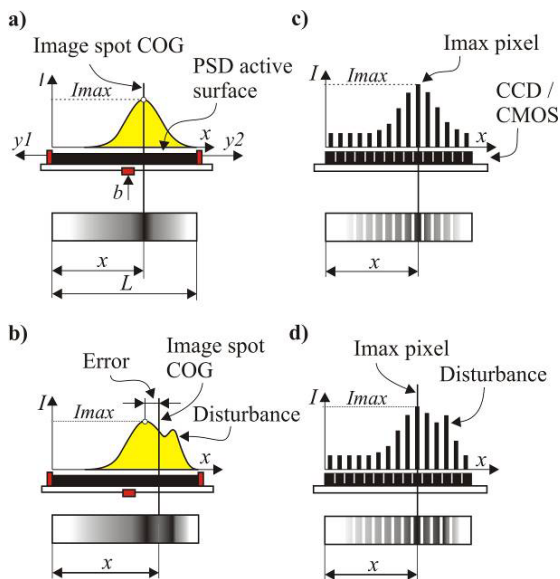


**Figure 2. Operating principle of analogue (a, b) and digital (c, d) photo detector and their sensitivity to errors.**

The one-dimensional array has a light-sensitive elements or photodiodes arranged in a line as shown in Fig. 2c. When these photodiodes are exposed to incoming light, the light is transformed into electrical charges whose size is proportional to the light intensity. At the time of registration, collected charges are transformed into a set of voltages that are directly proportional to the size of the charges, and thereby proportional to the intensity of light striking each pixel of the detector. Besides the space discretization (this type of detector is in fact an ordered set of pixels), the voltage output of each pixel is discretized in time and intensity. Therefore, this type of detector is essentially a digital device able to preserve complete information content of the imaged light spot, i.e., its space location, as well as its intensity profile (shown in Fig. 2d).

In general, digital photodetector can be realized either as charge coupled device (CCD) imager or as

complementary-metal-oxide-semiconductor (CMOS) imager. Besides the differences in underlying technology, the main difference between them is the way how they process and transfer data for each pixel. CCD process pixel data sequentially while CMOS imager process pixel data in parallel. It means that when exposure of particular pixel in CCD imager is complete, each pixel's charge packet is transferred sequentially to a common output structure and then processed and sent off-chip. In a CMOS imager, the charge-to-voltage conversion takes place in each pixel, i.e., immediately after shut-off signal processing is performed locally in parallel way. This difference in readout techniques has significant implications to sensor architecture, capabilities, limitations and overall performances.

Although PSD can handle data rates far greater than the photodiode arrays, and process these data on much simpler way (is especially a very important simple mechanism for very fast compensation of overall light-level changes), they are not so efficient in RCS thickness measurement. The ability of digital detectors to preserve and process the imaged spot profile using arbitrary complex algorithms, make this technology preferable in RCS thickness measurement task. Recent advances in CMOS technology, in particular improvements in signal to noise performances as well as the more synchronized shut-off function, enables digital detectors to run at high sampling frequencies too.

### 2.3 Surface reflectivity

Because triangulation operates by imaging the light reflected from the surface, a change in surface reflectivity will change the level or intensity of light reaching the detector. Reflectivity is influenced by several factors, including the color and surface waviness/roughness/texture of the object being measured, [3] and [4].

When a light beam hits the diffusive CR surface, a certain amount is transmitted through the medium, a certain amount is absorbed by the medium itself and the rest of light is reflected. If the reflection coefficient is designated by  $L\rho$ , the transmission coefficient by  $L\tau$  and the absorption coefficient by  $L\alpha$ , it is evident that the following must be satisfied:

$$L\rho + L\tau + L\alpha = 1. \quad (8)$$

Reflected light, that is of prime importance for optical triangulation, may be classified in three various types of reflection. Each of those three types of reflection is characterized by the geometric appearance of the light diffusion. These are the specular reflection share, the Lambert reflection distribution share and the share represented by Gaussian reflection diffusion.

Specular reflection is a reflection without diffusion and ideally follows the reflection law. Since the incident light is perpendicular to the diffusive surface, this component of the reflected light is not significant for laser proximity sensor. Moreover, under specific conditions, specular component can interfere with usable reflected components and generates reading uncertainties. For those reasons, the measuring systems

that are based on specular reflection differ in design concept [7].

The Lambert diffuse reflection refers to the case of uniform reflection that means that the luminance  $L$  of the reflected light is constant for different angles  $\theta$ , where  $\theta$  is measured from the surface's normal axis. In addition, the light intensity  $I$  of the reflected light follows the relation:

$$I_{\theta} = I_0 \cos \theta, \quad (9)$$

independently of the angle of incidence. White paper, projection screens and random rough surfaces have a very large share of Lambert reflection. A Lambert reflector is thus characterized by the fact that the reflected light is visible under the space angle of  $\pi$  steradians. In reality this angle is smaller and, as it is reported in [5] and [6], it is strongly proportional to the power spectral density of the target surface asperities height function. In general, the Lambert reflection diffusion share is far favorable for optical triangulation.

Gaussian reflection diffusion means that the reflected light basically follows the law of reflection, but the reflected light is more or less scattered around the reflection angle (side leakage). The light intensity of Gaussian diffuse reflection has a Gaussian scattering profile whose terminal points define the double beam angle  $\phi$ . Scattering angle is very seldom greater than  $25^{\circ}$ . Gaussian reflection share in some cases helps optical triangulation, but in general, it can cause some uncertainties, especially in case when PSD detector is used and diffuse target surface is inclined.

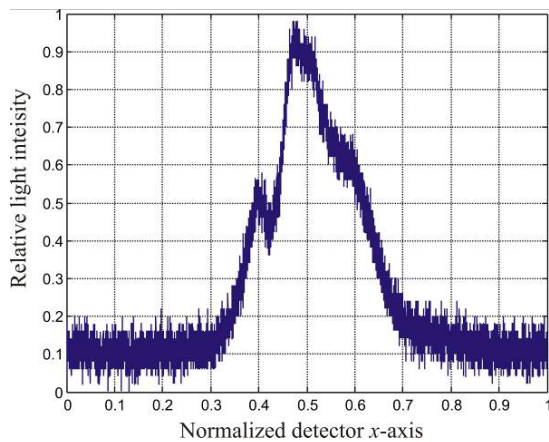


**Figure 3. Imaged light spot profile captured by 2048 pixel one-dimensional CCD photodiode array.**

Typical profile of imaged spot reflected from RCS sample surface is shown in Fig. 3. This profile is generated by one-dimensional photodiode array with 2048 sensing elements, i.e., pixels. It is clear that captured profile is noisy and significantly differs from theoretical Gaussian bell shaped profile which can be normally obtained under ideal measuring conditions and uniform properties of diffuse reflective target surface. Such profile mainly resulted from non uniform optical conditions of the measured sample and changes in surface reflectivity. CR has a highly structured surface composed of asperities at micro level and regular texture at macro level. The structure at the micro level is

generally termed as roughness, while the structure at the macro level is termed texture and waviness. The texture in this particular case is generated by underlying textile cords. Waviness is irregular macro feature of manufactured RCS caused by internal stresses which are, in general, the consequence of non uniformity of cord tension.

Gradual motion of the RCS surface in lateral direction, which typically occurs during the scanning motion, produces very dynamical changes in imaged spot profile. In Fig. 4 are shown successive light profiles captured by the same optical sensor as this one shown in Fig 3, when target RCS sample is moved incrementally in lateral direction with steps of  $100\mu\text{m}$ . The imaged spot profile can be distorted even greater in case when small shine areas exist in the RCS surface. These spots are easily generated when processed rubber compound is locally overheated due to unfavorable conditions of calendaring process. Each shine area behaves as small mirror which reflects significant part of the incoming laser beam into single direction. This reflected light component results in intensive distortion of imaged spot profile.

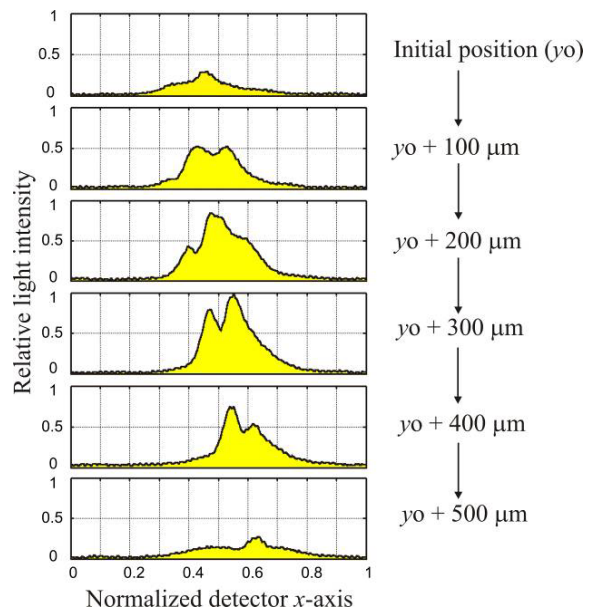


**Figure 4. Imaged spot profile variation during incremental lateral motion of target RCS surface (six successive steps of  $100\mu\text{m}$ , LP filtered).**

Under above described optical conditions accurate and fast triangulation in RCS measurements is a very demanding engineering task and special algorithms should be used in estimation of true distance of measured sample surface.

#### 2.4 CR surface inclination

In case of inclined diffuse target surface, i.e., when the angle of light incidence differs from  $\pi/2$ , two types of reading uncertainties can be generated. The first one is related to the distortion of reflected light intensity profile. Only in case when incidence angle is  $\pi/2$  the reflected light is entirely free of specular component and Gaussian component may be neglected. In other cases,

total reflection is composed of Lambert and Gaussian component. In RCS measurements the specular component are frequently present too. The result is a distorted image profile, which generates in that way measuring error.

The second type of reading uncertainties is so called light shadowing error, when diffuse reflected light is physically restricted, completely or partially, to reach detector or when the image light intensity is so weak to properly excite the detector. The presence of shadowing conditions most frequently generates reading dropouts.

RCS has textured surface of a corrugated form, i.e., regular waves that follows the cord pattern on a macro level (typical wavelength ranges from 1 to 3 mm). The RCS waviness appears for optical triangulation as a periodical change in inclination of diffuse target surface, providing nominal measuring conditions only within the narrow top area of each wave. Therefore, the most reliable measuring results can be expected in these areas only.

### 3. EFFECTIVE THICKNESS

RCS thickness is difficult to define because RCS is compressible and its surface is highly textured. Filtering of measured data in a way defined by ISO 13565-1: 1996 and ISO 11562: 1996 is in general not applicable due to potential presence of fragmented or incomplete vector of measured data. Also, highly textured surfaces measured by triangulation sensor has inherent source of reduced precision on sloped and valley areas as described before. In order to provide reliable method capable to be effective under these circumstances in this paper is proposed effective thickness estimation method based on statistical characterization of RCS surface.

Surface characterization techniques can be classified as statistical methods, spectral height correlation or auto-correlation methods, or fractals and self-similarity methods [7, 8]. In dimensional metrology surface characterization is mainly performed using statistical three-layer surface model and linearized material ratio curve [9]. Within this approach the rough surface is decomposed on the layer which contains protruding peaks, the layer which contains the core material of roughness profile, and the valleys layer.

Decomposition of rough surface on tree layers, and statistical characterization of each of them, can be used in RCS effective thickness estimation. Such characterization is closely related to the manufacturing process. Calendering is naturally slow and inertial process and consequently, statistical properties of the generated CR surface will change slowly in time. Therefore thickness estimation based on parameters of linearized material ratio curve can be performed with equal accuracy over continuously acquired sensory data, or the data which are fragmented.

Direct application of surface characterization based on material ratio curve in RCS thickness estimation is not possible. It must be extended to textured surfaces before. Moreover, some additional adaptations are necessary when thickness estimation is performed by two-sided measurement, since in this case the measured profile is obtained by superimposition of two different

surfaces, i.e., upper and bottom surface of RCS, each of them scanned by its own laser triangulation sensor (this will be discussed in more detail in the following text).

### 3.1 Surface characterization

For thickness measurement task it is important to determine, in percent, the material portion  $MR1$  that separates the protruding peaks from textured surface core profile.

If it is assumed that RCS thickness variation  $z(x)$  corresponds to the stationary Markov process [10], then the value of thickness for any lateral coordinate  $x$  belongs to the same distribution. In this case we assume Gaussian distribution  $N(\mu, \sigma)$ . This assumption is confirmed by experiments. Figure 5 shows the typical texture profile of CR sample scanned by laser proximeter with the sampling rate of 10 kHz and scanning speed of 50 mm/sec. The measurements are performed in laboratory conditions. It is clear that thickness variation  $z(x)$  of scanned texture profile is well correlated with normal distribution within the probability interval [0.05 0.95], and therefore CR surface can be considered as Gaussian surface.

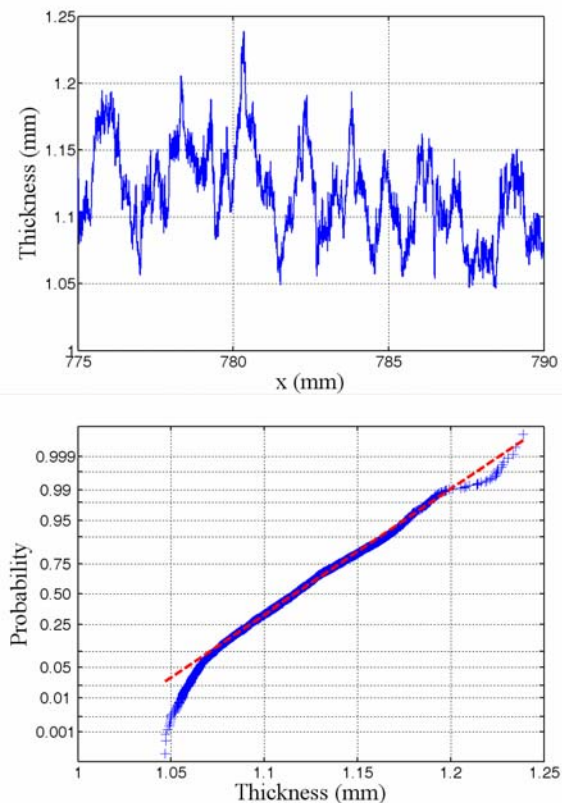


**Figure 5. Scanned texture of RCS sample measured from flat reference surface (up) and corresponding normal probability plot (down).**

Introducing so-called indicator function  $I$  meaning that:

$$I(x) = \begin{cases} 1 & \text{if } z(x) > \delta_E \\ 0 & \text{otherwise,} \end{cases} \quad (15)$$

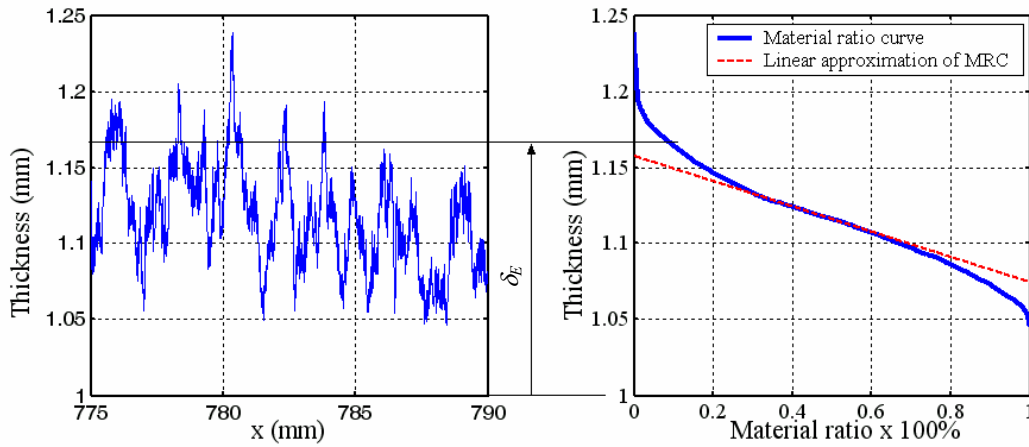


**Figure 6.** Example of measured RCS texture profile and corresponding material ratio curve with its smallest gradient linear approximation derived in accordance to proposed algorithm.

where  $\delta_E$  is height from arbitrarily chosen reference line, material portion  $Mr1$  in the interval  $x \in [0, L]$  can be defined using the following relation:

$$Mr1 = \int_0^L I(x) dx. \quad (16)$$

Expectation for such defined material portion is:

$$E(Mr1) = E\left(\int_0^L I(x) dx\right) = \int_0^L P\{z(x) > \delta_E\} dx \quad (17)$$

and since:

$$P\{z(x) > \delta_E\} = 0.5 - \Phi\left(\frac{\delta_E}{\sigma}\right), \quad (18)$$

it follows:

$$E(Mr1) = \left[0.5 - \Phi\left(\frac{\delta_E}{\sigma}\right)\right] L. \quad (19)$$

Mathematically, material ratio curve is equivalent to the cumulative distribution  $F(z)$  of RCS thickness variation in a given interval:

$$F(z) = \frac{df(z)}{dz} = \frac{1}{\sigma\sqrt{2\pi}} e^{-\frac{(z-\mu)^2}{2\sigma^2}}. \quad (20)$$

The difference is that the coordinate system is rotated and mirrored only (see Fig. 5).

The equivalent straight line that linearizes material ratio curve can be derived using similar approach as in ISO 13565, but instead of using secant, the proposed method is based on linear regression of the window that includes 40% of totally measured data points, or equivalently  $\Delta Mr = 40\%$ . Although it is computationally intensive such method of linearization is much more robust than the method based on secant.

The location of the core profile central axis is defined by the window which has the linear regression with the smallest gradient. Since the value of the gradient determines the width of the core profile,

selection of the smallest gradient is at the same time selection of the narrower core profile. The smallest gradient search algorithm can be easily performed by sliding the regression window iteratively, starting from  $Mr = 0\%$  and moving to the right. Contrary to the secant method the search algorithm for core profile central axis based on minimum gradient linear regression is very stable and insensitive to local irregularities that normally can occur in material ratio curve. This is very important for real time application.

Above described procedure of statistical surface characterization based on material ratio curve and three-layer texture representation is shown in Fig.6. The data used in Fig. 6 are the same as those used in Fig 5. Since they are well correlated to normal distribution, the shape of obtained material ratio curve is very similar to S shape of the normal cumulative distribution function. The upper limit which separates the protruding peaks from texture core profile is determined by thickness value of linear regression line for  $Mr = 0\%$ , while the lower limit which separates the deep valleys is determined by thickness value for  $Mr = 100\%$ .

In case of ideal Gaussian variation of RCS surface texture, the central region is located at the interval  $Mr = [30\%, 70\%]$  and the smallest slope of corresponding linear approximation can be derived directly from (20):

$$k = -\sigma\sqrt{2\pi}, \quad (21)$$

which further leads to the analytical formulation of material ratio curve linear approximation:

$$\delta = -\sigma\sqrt{2\pi}(Mr - 0.5) + \mu. \quad (22)$$

If core profile of RCS surface texture is determined by  $Mr = 0\%$ , and  $Mr = 100\%$ , and consequently core boundaries can be defined directly from (22):

$$\delta_{CORE} = \left[\mu + \frac{1}{2}\sigma\sqrt{2\pi}, \mu - \frac{1}{2}\sigma\sqrt{2\pi}\right]. \quad (23)$$

It is important that ideal Gaussian surface statistical characterization is completely defined through two parameters, i.e., mean value and variance of measured data. This is true regardless of their completeness. Only

what is necessary to be satisfied is the size of collected data which must be sufficient enough to estimate normal distribution parameters for adopted degree of certainty. The material ratio curve and core profile boundaries for ideal Gaussian surface are shown in Figure 7.

### 3.2 Statistical definition of effective thickness

Normally, effective thickness is the distance between reference surface that supports RCS sample and upper limit of RCS surface core profile, or equivalently, the intersection point of linearized material ratio curve (22) with abscise  $Mr = 0\%$ . In case that RCS surface is ideal Gaussian surface, effective thickness can be analytically expressed by the following equation:

$$\delta_{EFF} = \mu + \frac{1}{2}\sigma\sqrt{2\pi}. \quad (24)$$

Introducing (24) into (19) corresponding material portion  $Mr1$  can be calculated:

$$Mr1_{EFF} = 0.5 - \Phi\left(\frac{1}{2}\sqrt{2\pi}\right) = 0.105. \quad (25)$$

It means that 10.5% of material ratio belongs to protruding peaks. By selecting other values of abscise, i.e.,  $Mr$  greater than 0%, one can calculate lower effective thickness and greater rejected material portion. Physically, this is related to compressibility of the RCS. Any mechanical gauge applies some pressure and therefore affects the thickness. Percentage of rejected material portion which is leaved to protruding peaks layer may be interpreted as rising up of contact force in contact measurement methods (thickness measurement by micrometer caliper gauge for instance, which is standard measuring instrument in manual thickness measurement, applies precisely defined pressure to the contact foot with standardized diameter).

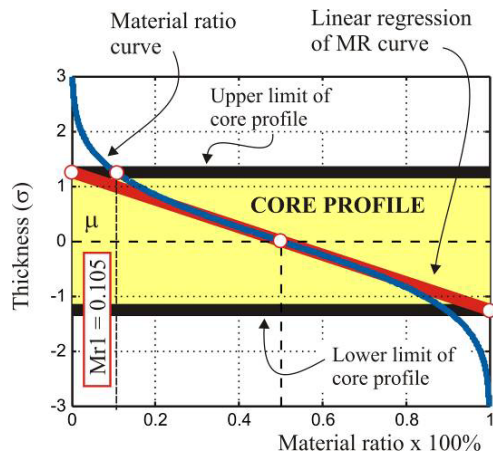


**Fig.7: Standardized material ratio curve for ideal Gaussian texture ( $\mu = 0$  mm, which gives  $k = -2.5066\sigma$ ,  $\delta_{core1} = 1.2533\sigma$ ,  $\delta_{core2} = -1.2533\sigma$ ).**

By varying value of material ratio  $Mr1$  specific kind of filtering is performed. This filtering removes outlying data points, peaks and debris, leaving only core material that is of primary interest in thickness measurement. Also, it rises up the accuracy and robustness of entire measurement process.

In case that material ratio curves are defined for both, upper and lower surface, the equivalent thickness

can be defined as a distance between upper limits of the texture core profiles of two RCS surfaces. It means that two material ratio curves  $F1(z)$  and  $F2(z)$  were estimated from sensory data and their linear approximations are derived using relation (22).

Proposed surface characterization method for RCS effective thickness estimation may be interpreted as a method for robust recovering of lost information content, caused by shadowing effect in differential laser triangulation scanning of RCS surface. Therefore, it is a good solution for solving the problem of extensive dropout rate which frequently appears in RCS thickness measurement based on commercially available single triangulation laser proximity sensors. Moreover, in proposed surface characterization method, data which belong to valleys are not necessary in effective thickness estimation. This is of high importance, because even if laser triangulation sensor is able to acquire valid measurements, such measurements are critical in respect to achieved accuracy (influence of distorted image profile as discussed before).

### 4. CONCLUSION

The outline of advanced technology for in-process RCS thickness measurement by laser triangulation is presented. Analytical model of laser triangulation and the most critical problems in distance measurements of the objects having highly textured surfaces are considered in details. Based on this analysis the new method for noncontact thickness estimation of RCS is proposed. This method is based on three-layer structured surface textured and statistical characterization of these layers. It is proved analytically and by experiments that the RCS texture is Gaussian type of texture, which further enables accurate and robust thickness estimation only using identified parameters normal distribution of scanned RCS surface texture. Results obtained from laboratory experiments show that the new method is capable to replace the existing methods based on radiation sensors, with better measuring properties and no environmental risk.

### REFERENCES

- [1] Schwenke, H. et al.: Optical Methods for Dimensional Metrology in Production Engineering, Annals of the CIRP, 51/2, pp. 685-699, 2002.
- [2] Luxon, J.T., Parker, D.E.: *Industrial Lasers*, Prentice-Hall, Englewood Cliffs, New York, USA, 1985.
- [3] Ogilvy, J.A.: *Theory of wave scattering from random rough surfaces*, Hilger, Bristol, 1991.
- [4] Stover, J.C.: *Optical scattering: measurement and analysis*, SPIE Optical Engineering Press, Bellingham, Washington, 1995.
- [5] Lehman, P., Goch, G.: Comparison of Conventional Light Scattering and Speckle Techniques Concerning an In-Process Characterization of Engineered Surfaces, Annals of the CIRP, 49/1, pp. 419-422, 2000.

- [6] De Shiffre, L. et al.: Quantitative Characterization of Surface Texture, *Annals of the CIRP*, 49/2, pp. 635-652, 2000.
- [7] Stout, K.J.: *Development of Methods for the Surface Characterization of Roughness in Three Dimensions*, Penton Press, London. 2000.
- [8] Ariano, I., Kleist, U., Barros, G.G., Johanson, P.A., and Rigdahl, M.: Surface Texture Characterization of Injection-Molded Pigmented Plastic, *Polymer Engineering and Science*, Vol. 44/9, pp. 1615-1626, 2004.
- [9] Zhang, G.X. et al.: A System for Measuring High-Reflective Sculptured Surfaces Using Optical Noncontact Probe, *Annals of the CIRP*, 50/1, pp. 369-372, 2001.
- [10] Haggstrom O.: *Finite Markov Chains and Algorithmic Applications*, Cambridge University Press, 2002.

---

**МЕРЕЊЕ ДЕБЉИНЕ ГУМИРАНОГ КОРДА  
ПРИМЕНОМ ЛАСЕРСКЕ ТРИАНГУЛАЦИЈЕ  
– Део I: Технологија**

**Петар Б. Петровић**

У раду је презентираан концептуални оквир технологије мерења еквивалентне дебљине гумираног корда применом оптичке триангулације. Детаљно је изложен аналитички модел ласерског проксиметра и разматрани су основни проблеми везани за функционисање и примену ласерске триангулације у мерењу дистанце објеката са изразито текстуираним површином која поседује неуниформна оптичка својства. Предложена је нова метода која омогућава робусну и високопрецизну естимацију ефективне дебљине гумираног корда. Ова метода је базирана на структурирању површи на три слоја и статистичкој карактеризацији ових слојева. Показано је да текстура гумираног корда одговара класи Гаусових површи, на основу чега је могуће прецизно и врло робусно израчунавање еквивалентне дебљине само на основу естимираних параметара нормалне расподеле скенираног узорка површи. Лабораторијски експерименти су потврдили практичну употребљивост ове методе и створиле реалне основе за развој нове технологије мерних система који ће моћи да замене конвенционална решења базирна на сензорима са природним или вештачким изворима радиоактивног зрачења.